Design of a Specific Phenyllactate Dehydrogenase by Peptide Loop Exchange on the *Bacillus stearothermophilus* Lactate Dehydrogenase Framework†

Helen M. Wilks,* Kathleen M. Moreton, David J. Halsall, Keith W. Hart, Richard D. Sessions, Anthony R. Clarke, and J. John Holbrook

Molecular Recognition Centre and Department of Biochemistry, University of Bristol School of Medical Sciences, Bristol BS8 1TD, U.K.

Received November 15, 1991; Revised Manuscript Received May 28, 1992

ABSTRACT: Restriction sites were introduced into the gene for *Bacillus stearothermophilus* lactate dehydrogenase which enabled a region of the gene to be excised which coded for a mobile surface loop of polypeptide (residues 98–110) which normally seals the active site vacuole from bulk solvent and is a major determinant of substrate specificity. Oligonucleotide-overlap extension (using the polymerase chain reaction) was used to obtain double-stranded DNA regions which coded for different length and sequence loops and which also contained the same restriction sites. The variable length and sequence loops were inserted into the cut gene and used to synthesize hydroxyacid dehydrogenases with altered substrate specificities. Loops which were longer and shorter than the original were made. The substrate specificities of enzymes with these new loops were considerably altered. For many poor enzyme–substrate pairs, the effect of fructose 1,6-bisphosphate on the steady-state kinetic parameters suggested that the substrate was mainly bound in a nonproductive mode. With one longer loop construction (BL1), activity with pyruvate was reduced one-million-fold but activity with phenylpyruvate was largely unaltered. A switch in specificity (k_{cat}/K_M) of 390 000-fold was achieved. The 1700:1 selectivity of enzyme BL1 for phenylpyruvate over pyruvate is that required in a phenyllactate dehydrogenase to be used in monitoring phenylpyruvate in the urine of patients with phenylketonuria consuming an apparently phenylalanine-free diet.

Rational redesign (Dunn et al., 1991) has so far resulted in the protein framework from *Bacillus stearothermophilus* NAD^+-dependent lactate dehydrogenase being converted to an active malate dehydrogenase (Wilks et al., 1988), an $NAD^+/NADP^+$-dependent LDH[1] (Feeney et al., 1989), and a broad specificity 2-hydroxyacid dehydrogenase (Wilks et al., 1990). These hydroxyacid dehydrogenases, in the reverse (but thermodynamically favorable) direction, can potentially be used in a NADH-based assay to determine the concentrations of the corresponding 2-ketoacids in physiological fluids. Inborn errors in the metabolism of amino acids in the newborn lead to a buildup of the ketoacid by deamination of the nontransformable amino acid: phenylpyruvate in many cases of phenylketonuria and 2-ketoisocaproate in the case of maple syrup urine disease [see Wu (1991) for a recent review]. Thus, the ability to specifically assay for the different 2-ketoacids in either serum or urine offers the potential to distinguish between the different inherited diseases in a way which could be easily integrated into modern automated analyzers or biosensors. Alternatively, it may be possible to develop specific amino acid dehydrogenases for phenylalanine (Wendel et al., 1989; Hummel et al., 1988). In this paper, we use knowledge of the LDH specificity pocket (Dunn et al., 1991) to redesign an enzyme normally specific for pyruvate to give one specific for phenylpyruvate. The best construction had a k_{cat}/K_M for phenylpyruvate 1700 times better than for pyruvate, while the wild-type enzyme has k_{cat}/K_M for pyruvate 230 times better than for phenylpyruvate: a switch in specificity of 390 000-fold.

† The work was supported by the Science and Engineering Research Council (U.K.) and Genzyme (U.K.) Ltd.

* Author to whom correspondence should be addressed.

[1] Abbreviations: LDH, L-lactate dehydrogenase; TEA, triethanolamine hydrochloride; FBP, fructose 1,6-bisphosphate.

MATERIALS AND METHODS

Mutagenesis To Construct SacII and XbaI Sites at Either End of the Gene Coding for the Wild-Type Active Site Loop. A 54-mer oligonucleotide was used to direct mutagenesis to introduce unique restriction sites (*Sac*II and *Xba*I) at either end of the active site loop (amino acids 98–110) using the wild-type pLDH41 template (Barstow et al., 1986). The mutagenic oligonucleotide was 5′GTCCACAAGGTCTAGACGCGTCTCGCCCGGTTTTTGGTTGGCGCCCGCGGTAATGACAAC3′. The annealing, chain extension, and cloning were as described by Clarke et al. (1986). Mutants were identified by making mini-preps and restricting with *Sac*II and *Xba*I. Mutant mini-preps were restricted with *Eco*RI and *Xho*I, and the small fragment was subcloned into pLDH41 containing the Ala235Gly, Ala236Gly mutation of LDH which had also been restricted with *Eco*RI and *Xho*I and from which the small fragment had been removed (Wilks et al., 1990). The resulting plasmid (pLDHrs) was transformed into competent *Escherichia coli* TG2 cells. The whole sequence was redetermined using a Du Pont Genesis 2000 automatic sequencer and showed that the correct loop sequence and helix α-2G sequences had been inserted. Partial DNA sequences of the wild-type gene and the mutant with inserted restriction sites in the specificity loop regions are shown in Figure 1.

Generation of Double-Stranded DNA Loop Fragments by Oligonucleotide-Overlap Extension. Each pair of overlapping oligonucleotides (20 μM each) was subjected to 30 cycles of annealing and extension (94 °C, for 1 min, cool to 45 °C in 2 min, 45 °C for 1 min, heat to 72 °C in 1 min, 72 °C for 1 min), in 50 μL containing 0.05 M KCl, 10 mM Tris, pH 8.3, 1.5 mM $MgCl_2$, 0.01% gelatin, 200 μM for each dNTP, and 2.5 units of Taq DNA polymerase. The double-stranded DNA product was purified and then cut with *Sac*II and *Xba*I

0006-2960/92/0431-7802$03.00/0

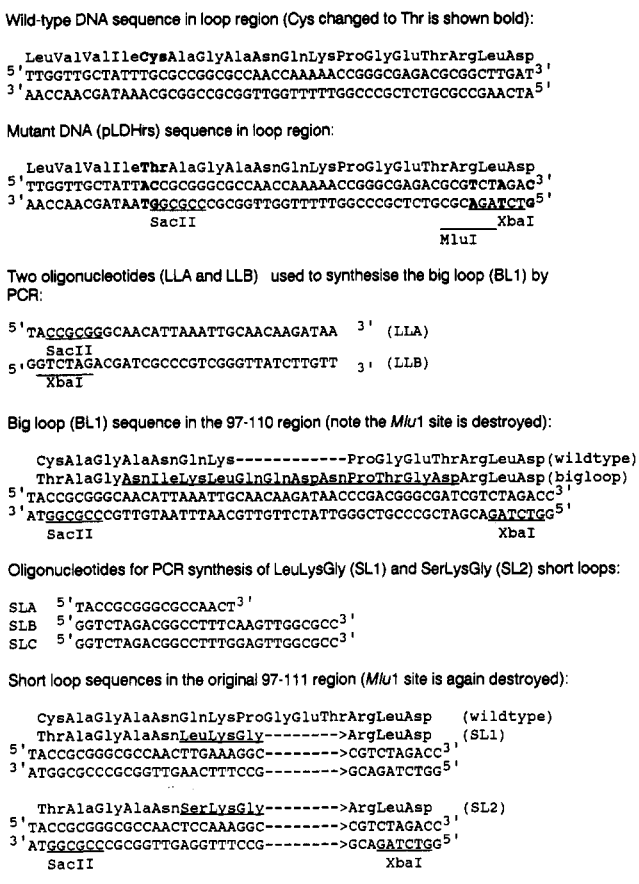

FIGURE 1: Comparison of the protein and DNA sequences of wild-type *B. stearothermophilus* LDH in the loop (93–111) region of the wild type, the mutant with *Sac*II and *Xba*I restriction sites at either end of the loop, and the variable loop sequences derived from them. Oligonucleotides LLA and LLB were used in the polymerase chain reaction oligonucleotide-overlap extension method to synthesize the DNA coding for the big loop, BL1, protein. Oligonucleotide SLA with SLB and SLC was used to synthesize DNA coding for the SL1 and SL2 proteins respectively.

before ligating it into pLDHrs which had been cut with the same enzymes. The ligated products were restricted with *Mlu*I to cleave any wild-type plasmid pLDHrs. The DNA was purified, microdialyzed, and used to transform *E. coli* TG2 cells by electroporation. Transformed cells were selected for ampicillin resistance. Ten such colonies were picked and plasmid DNA purified from overnight cultures. The presence of mutant loops was confirmed by resistance to *Mlu*I digestion.

Purification of the Standard (WTrs), Big (BL1), and Short (SL1 and SL2) Loop Mutants of LDH on the ^{235,236}GG Protein. Normal, short, and big loop mutants were purified by ion-exchange chromatography on Q-Sepharose Fast Flow. Overnight cultures (1 L) were centrifuged, and the packed cells were resuspended in 50 mM triethanolamine, pH 6.0. The cells were sonicated, and the debris was removed by centrifugation. The protein in the supernatant was precipitated by the addition of 65% ammonium sulfate. The precipitate was spun down and resuspended in 50 mM triethanolamine, pH 6.0, and dialyzed against the same buffer. After dialysis, NADH and FBP were added to the protein to final concentrations of 5 mM and 10 mM, respectively, before loading onto the oxamate–Sepharose column which had been pre-equilibrated with 50 mM triethanolamine, pH 6.0, 0.3 mM NADH, and 5 mM FBP. After unbound protein was eluted with column buffer, mutant LDH was eluted with 50 mM triethanolamine, pH 9.0, 0.3 M NaCl. The LDH-containing eluate was precipitated with 65% ammonium sulfate and then resuspended in and dialyzed against 50 mM triethanolamine, pH 7.5. The protein was then loaded onto the Q-Sepharose Fast Flow column and eluted with a salt gradient. LDH eluted at a concentration of 0.25 M NaCl. All proteins were judged to be greater than 99% pure from the intensity of Coomassie blue staining on an SDS Phast gel. The yield of pure enzyme was usually 0.2 g/L of original broth.

Steady-State Kinetics. The enzymes all followed simple Michaelis–Menten kinetics at noninhibitory concentrations of α-ketoacids, and initial rates of A_{340nm} decrease versus substrate concentration data were fitted to an hyperbola using the nonlinear regression contained within Grafit 2 (Leatherbarrow, 1990). The buffer was 20 mM Bis-Tris, pH 6, 50 mM KCl with, when used, 5 mM FBP at 25 °C. Note this is a different and probably better pH 6 buffer than used in much of the previous work from this laboratory and could result in small quantitative differences from previously reported kinetic parameters. Calculations of k_{cat} depended on the protein concentration determined from A_{280nm} using an absorbance of 0.91 for the 1 mg/mL protein solution in a 1 cm path and M_r = 33 000.

RESULTS AND DISCUSSION

Design Considerations

The mechanism by which LDH distinguishes different substrates is the ability of the substrate to fit into a proton-impermeable, fixed-size internal vacuole which is formed when a mobile surface polypeptide loop closes down onto the protein surface (Figure 2a). Loop closure is only possible over suitably small and singly negatively charged substrates. Closure also triggers catalysis since the underside of the loop carries Arg109—the residue which reduces the transition-state energy by 6 kcal through polarization of the 2-keto function of the substrate [see Holbrook et al. (1975) for a review and Dunn et al. (1991) for a recent update]. We decided to retain the catalytic Arg109 in all constructions, and particularly in the short loop versions where the loop was locked down (see Selection of Loop Sequences), as we expected this would give tight binding of substrate because the substrate-binding energy would not additionally have to drive loop closure, as it does in the wild-type enzyme (Dunn et al., 1991). The complex of enzyme, coenzyme, and substrate analogue is rigid and contains many low mobility waters whose hydrogen bonds serve to form a network stabilizing the 5 amino acids which hold the substrate analogue on the catalytic pathway by 7 hydrogen bonds. In the complex of just enzyme and coenzyme, the gap between helix α-2G and the loop opens and many fewer low mobility waters are seen in the crystal structure. Experimentally, it is observed that enzymes which have poor loop to helix α-2G contact are limited by slow hydride transfer (Dunn et al., 1991).

Selection of Loop and Other Sequences

The method to make the new loop constructions, one very big and two short ones, was to insert restriction enzyme sites at either end of the DNA coding for the loop region, to cut out the DNA coding for the wild-type loop region, and then to religate with synthetic DNA designed to code for the new loop regions. Insertion of an *Xba*I site close to the region coding for Arg109 also resulted in an *Mlu*I site close to Thr108. This additional site was useful since it was destroyed in transformants and enabled their easy distinction from the wild-type gene (see Figure 1 for detailed sequences). The wild-type amino acid sequence could be retained (including the catalytic Arg109). The construction of the *Sac*II restriction

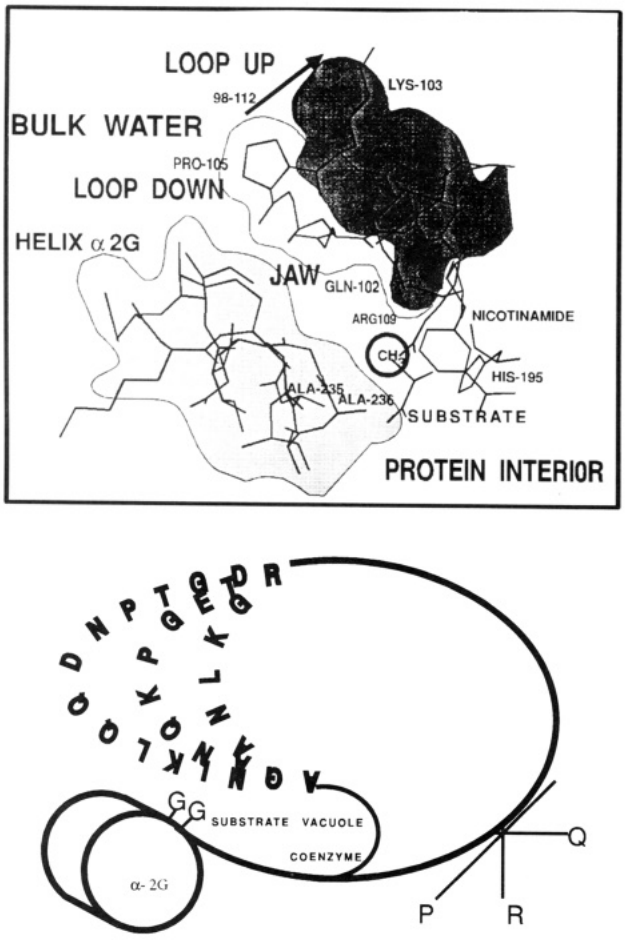

FIGURE 2: Diagrams to illustrate loop design on the LDH active site vacuole. (a, top) The internal vacuole which determines the space available to the substrate is formed after the loop (98–110) closes down onto helix-2G (Dunn et al., 1991). The light shading is a projection of the surfaces defined by helix α-2G and the loop β-D to α-D/E in the ternary (active) complex. The dark shading is the opened position of the loop. (b, bottom) Regular, small (SL1 shown), and big (BL1) polypeptide loops were inserted between Asn101 and Arg109 on a more open framework than that of wild type containing the $AA^{235,236}GG$ substitution (Wilks et al., 1990) and the mutation C97T. These constructions are called WTrs, BL1, SL1, and SL2 in Table I. P, Q, and R are three orthogonal axes from the center of the tetramer which enable the rotations to generate the other three subunits from that shown.

site required Cys97 be changed to threonine. Molecular graphics modeling suggested that change was not likely to alter substrate specificity, and many other natural LDHs have threonine at this position and are active.

The loops were added into the gene which coded for a previously designed, broad specificity 2-hydroxyacid dehydrogenase which was the wild-type *B. stearothermophilus* LDH amino acid sequence containing the $^{235,236}AA \rightarrow {}^{235,236}GG$ mutations (Wilks et al., 1990). This change of two alanines to two glycines had been previously used to increase space in the vacuole adjacent to the substrate side chain and had resulted in enzymes which were better than the wild type for larger substrates (Holbrook et al., 1989). These ideas are presented diagrammatically in Figure 2b.

Calculations were implemented by DISCOVER and INSIGHT version 2.5 (Biosym Technologies, San Diego, CA). INSIGHT contains a loop-building module which was used to search a particularly accurate subset (structures of resolution less than 2 Å) of the Brookhaven Protein Data Bank of protein three-dimensional structures for tripeptide loops which would best

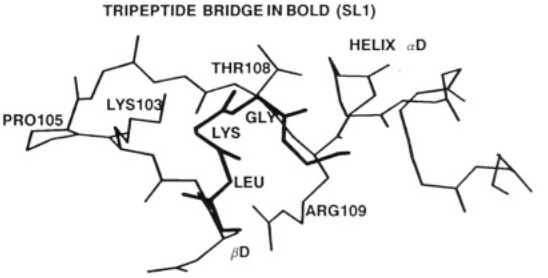

FIGURE 3: Design of the short loop constructions. A superposition of one 3-amino acid loop (in bold) used to bridge between the Cα atoms of Arg109 and Asn101 of the coordinates of *B. stearothermophilus* LDH quaternary complex with NADH, oxamate, and fructose 1,6-bisphosphate crystallized from PEG6000 (Wigley et al., 1992). Because Arg109 is very important for catalysis and polarizes the substrate >C=O (Clarke et al., 1986), particular care was taken to ensure that the shorter loops could be inserted without distorting the Ramachandran angles of the backbone as it entered and left Arg109. The conformation of the wild-type loop is that in a ternary complex. In the open structure (dark shading in Figure 2a), the tripeptide is too short by 2.4 Å to bridge between the Cα of Asn101 and Arg109.

fit between the Cαs of Asn101 and Arg109 and where the flanking five peptide bonds would superimpose well on the authentic LDH ternary complex (loop down) Cα backbone [coordinates from Wigley et al., (1992)]. The best match was by a Lys-Leu-Gly bridge. The candidate loops found by the search program were then further evaluated by modeling them into the original LDH structure on the graphics to optimize the match of the side chains to the new environment (see Figure 3). The surface exposure calculation of DISCOVER predicts that the short bridge opens the active site to water when it contains only coenzyme and a small substrate such as pyruvate. Large aromatic pyruvate derivatives such as phenylpyruvate have sufficiently bulky side chains to themselves seal the vacuole from the solvent. The enzyme was expected to be a very poor catalyst with small substrates which could not provide a good seal to exclude rapdily exchanging bulk solvent water. The tripeptide loops finally made a lysine at their tip to better match the solvent-exposed environment in this region of the new loops. The two shorter loops constructed (counting from Gly99 to Arg109) were (SL1) GANLKGR and (SL2) GANSKGR. The glycine at old position 108 was inserted to enable any shortcomings in design to be compensated for by local conformational mobility. Strain in the apo and binary structures was thought less likely to result in reduction of catalytic rate since these are only short-lived intermediates on the catalytic pathway. The tripeptides were selected to bridge between Cαs of residues 101 and 109 in the "loop down" (ternary complex) LDH structure. They were too short by 2.4 Å to bridge across in the apo or binary (loop up) structures. Short loops were thus predicted to considerably stabilize the loop down structure—with the catalytic Arg109 permanently directed into the active center.

The big loop (BL1) was modeled on the graphics, and the model showed that increasing the length of the regular loop by 4 residues would cause the new loop to bulge out and away from helix α-2G to create a vacuole which favored very large substrate side chains. With pyruvate present, a model of the loop had sufficient room for many extra solvent water molecules.

Properties of the New Loop Constructions

Before the properties of the constructs are described in detail, it is useful to note the conventional numbering used for LDH

Table I: Steady-State Kinetic Parameters of Some Loop Exchange Mutants[a]

substrate	parameter	wild type		235/6GG	WTrs		BL1		SL1		SL2	
		+FBP	-FBP	+FBP	+FBP	-FBP	+FBP	-FBP	+FBP	-FBP	+FBP	-FBP
pyruvate	k_{cat} (s^{-1})	250	250	167	60	19	0.2	0.05	0.2	0.1	0.07	0.04
	K_m (mM)	0.06	2	4	3.5	100	42	50	0.08	2.0	0.065	0.5
	k_{cat}/K_M ($M^{-1}\cdot s^{-1}$)	4.2×10^6	5×10^4	4.2×10^4	1.7×10^4	190	4.7	1	2.5×10^4	50	1.1×10^2	80
ketocaproate	k_{cat} (s^{-1})	29		240	88	12	6	0.3	0.8	0.07	0.1	0.1
	K_m (mM)	3.4		5.6	5.8	30	20	27	16	20	25	60
	k_{cat}/K_M ($M^{-1}\cdot s^{-1}$)	8.5×10^3		4.2×10^4	1.5×10^4	400	300	11	50	3.5	4	1.6
ketoisocaproate	k_{cat} (s^{-1})	0.33		1.74	1.8	0.2	0.3	0.06	0.07	0.01	0.9	0.08
	K_m (mM)	6.7		15	4	28	18	32	20	40	25	30
	k_{cat}/K_M ($M^{-1}\cdot s^{-1}$)	50		110	450	7.1	17	1.9	3.5	0.25	36	2.6
phenylmethylpyruvate	k_{cat} (s^{-1})	6		7	6	0.8	1.0	0.1	0.03	0.002	0.2	0.01
	K_m (mM)	0.6		13	4	12	7	12	4	4	4	4
	k_{cat}/K_M ($M^{-1}\cdot s^{-1}$)	1×10^4		540	1.5×10^3	67	140	8.3	7.5	0.5	50	2.5
phenylpyruvate	k_{cat} (s^{-1})	32.7		54	58	4	40	6	20	10	100	20
	K_m (mM)	1.8		4.5	6	21	5	100	11	80	3	20
	k_{cat}/K_M ($M^{-1}\cdot s^{-1}$)	1.8×10^4		1.2×10^4	9.6×10^3	190	8×10^3	60	1.8×10^3	125	3.3×10^4	1×10^3

[a] Repeat determinations of K_M were within ±10% of the values shown. K_M values >50 mM are less certain because of the high salt concentration and large absorbance of the solutions.

sequences, particularly in the region of the specificity loop. Note there is no residue numbered 104:

```
97  98  99 100 101 102 103 105 106 107 108 109 110
Cys Ala Gly Ala Asn Gln Lys Pro Gly Glu Thr Arg Leu
```

Three regular-length loop constructions are to be mentioned: the wild-type (WT) sequence (see above), the WT sequence but constructed on the framework with an enlarged catalytic vacuole due to the mutations A235G and A236G (235/236GG) (Wilks et al., 1990), and a construction containing the wild-type sequences from 98 to 110 but with the mutation Cys97Thr and the mutations A235G,A236G (WTrs). Three constructions with different length specificity loops are made on the WTrs framework: the big loop (BL1) construct with the WT (and WTrs) loop in the 99–109 region expanded from GANQKPGETR by 4 residues to GNIKLQDNNPTGDR and two loops shortened by 3 residues in the 99–109 region; SL1 being WTrs with the specificity loop GANLKGR and SL2 being WTrs with the specificity loop GANSKGR.

The Enlarged Vacuole ($^{235,236}AA \rightarrow {}^{235,236}GG$) with the C97T Mutation. The regular loop built on the ^{235,236}AA → ^{235,236}GG framework containing the C97T mutation was required to generate a *Sac*II restriction site in the gene at the start of the specificity loop coding region (WTrs). The expressed enzyme had a pattern of enzymic properties against the panel of substrates which is qualitatively similar to those of the ^{235,236}GG framework on which it was constructed (Figure 4). Thus, the idea that exchanging cysteine-97 for threonine would be enzymically neutral was reasonably fulfilled. As can be seen in Table I, there was some slight reduction in k_{cat} from 170 s^{-1} to 60 s^{-1}. An unexpected benefit from removal of the cysteine was that the overexpressed protein now ran as a single band on sodium dodecyl sulfate Phast gels which had not been subjected to pre-electrophoresis (as opposed to the wild-type C97-containing proteins which gave two bands under these conditions; results not shown).

Truncated Loops. Both the short loop constructions had some properties hoped for in the original design (Table I). The K_M for pyruvate was remarkably low (65–80 μM) for a pocket which now had too few residues to effectively seal against bulk water; substrate binding in the wild-type enzyme is achieved by hydrogen bonds to residues which form a network based on low mobility water (Dunn et al., 1991), and mobile water was thus expected both to reduce k_{cat} and, by providing alternate hydrogen bond partners, to also increase K_M. That

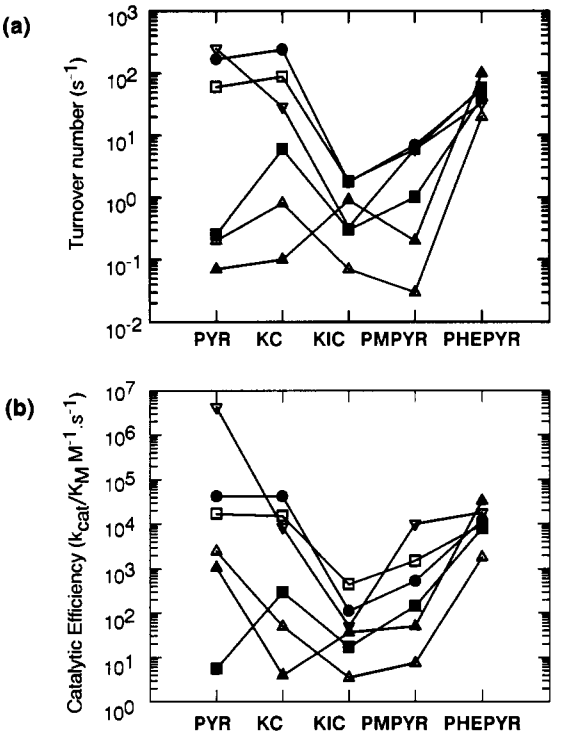

FIGURE 4: Log plots of (a) the maximum rate (k_{cat}) and of (b) the catalytic efficiency (k_{cat}/K_M) for the LDH constructions. Results for the wild type and the 235/236GG mutant are from Wilks et al. (1990). WTrs is the 235/236GG framework with Thr97 replacing Cys97 to create the *Sac*II site in the gene. The sequences of the big (BL1) and the two short loops SL1 and SL2 are in Table I. PYR is pyruvate, KC is ketocaproate, KIC is ketoisocaproate, PMPYR is phenylmethylpyruvate, and PHEPYR is phenylpyruvate. Symbols: (▽) WT, (●) 235/236 GG, (□) WTrs, (■) BL1, (△) SL1, (▲) SL2.

the low K_M was due to tight binding (as opposed to a kinetic term in K_M) was confirmed by measuring the K_i for oxamate (a true dissociation constant) and finding that it was 550 μM both in wild type and in SL2 (without FBP). This conclusion is also supported by the observation that both of these mutants were retained on an oxamate–agarose affinity column in the presence of NADH. There are two possible opposing effects on K_M in the shortened loop constructions. A larger K_M was expected from increased mobile water accessibility, whereas better binding was expected from locking Arg109 into the active site and thus preforming the substrate binding site. The very low k_{cat} was as expected from our previous experience with wild-type and mutant constructions where a mismatch

between substrate structure and the vacuole in the framework does not enable the catalytic pathway [as defined in Dunn et al. (1991)] to be shielded from mobile solvent water. Neither of the short loop constructs was very effective as a catalyst for the aliphatic substituted pyruvates tested. However, for phenylpyruvate the k_{cat} was high and for SL2 was increased to 100 s^{-1}—some 3 times better than the original wild-type *B. stearothermophilus* LDH, which itself is the best of the eukaryote and bacterial enzymes which have been tested against phenylpyruvate. This is yet one more example of enzyme design being able to better natural enzymes for activity against unnatural substrates (Clarke et al., 1991).

It has been shown (Hart et al., 1987) that the effect of FBP on both k_{cat} and K_M can diagnose the presence of large proportions of nonproductive enzyme–substrate complexes (Fersht, 1977) in mutant LDH constructions. For enzyme–substrate pairs where K_M is dominated by nonproductive binding, the effect of tightening the productive mode of substrate binding by adding FBP is (counter to intuition) to increase the measured k_{cat} with little effect on K_M. Where most of the substrate is bound productively (as in the wild-type enzyme, Table I), addition of FBP gives a 10–100-fold reduction in measured K_M with little or no change in k_{cat}. On the basis of this criterion, it is seen that most poor substrates bind to SL1 and SL2 nonproductively. As expected for good substrates and from the design ideas, the bulk of the side chain of phenylpyruvate ensures that most (but not all) is bound productively, both in the big and in the short loop constructions. It is clear that although selection against pyruvate was very successful, only SL2 of the varied loop structures resulted in an improved k_{cat}/K_M for the larger substrates.

The Enlarged Loop. The design expectation that the large loop would by its hydration of the catalytic pathway (Dunn et al., 1991) in the presence of only small substrates select against small substrates is fulfilled by the new construction (Table I). The k_{cat}/K_M for the small substrate, pyruvate, is reduced from 4.2×10^6 M^{-1} s^{-1} to just 4.7 M^{-1} s^{-1}. The k_{cat}/K_M for the larger phenylpyruvate is only slightly decreased from 1.8×10^4 to 8×10^3 M^{-1} s^{-1}. Had the design been perfect, we should have expected a modest increase in k_{cat}/K_M for the larger substrate. This suggests further, perhaps random, variation of the loop length and sequence could give improved catalysis for the larger substrates. When evaluated as a diagnostic enzyme, the "big loop" construction was much improved: it had k_{cat}/K_M for phenylpyruvate 1700 times better than for pyruvate compared to the wild-type enzyme which has k_{cat}/K_M for pyruvate 230 times better than for phenylpyruvate. A switch in specificity of 390 000-fold was achieved. The 1700:1 selectivity for phenylpyruvate over pyruvate demonstrates that this design idea is a route to a part synthetic enzyme suitable for the specific measurement of phenylpyruvate in physiological fluids (Holbrook et al., 1992).

REFERENCES

Barstow, D., Clarke, A. R., Wigley, D., Holbrook, J. J., & Atkinson, T. (1986) *Gene 46*, 47–55.

Clarke, A. R., Wigley, D. B., Chia, W. N., Barstow, D., Atkinson, T., & Holbrook, J. J. (1986) *Nature 324*, 699–702.

Clarke, A. R., Wilks, H. M., Barstow, D. A., Atkinson, T., Chia, W. N., & Holbrook, J. J. (1988) *Biochemistry 27*, 1617–1622.

Clarke, A. R., Colebrook, S., Cortes, A., Emery, D. C. Halsall, D. J., Hart, K. W., Jackson, R. M., Wilks, H. M., & Holbrook, J. J. (1991) *Biochem. Soc. Trans. 19*, 576–581.

Dunn, C. R., Wilks, H. M., Halsall, D. J., Atkinson, T., Clarke, A. R., Muirhead, H., & Holbrook, J. J. (1991) *Philos. Trans. R. Soc. London, B 332*, 177–184.

Feeney, R., Clarke, A. R., & Holbrook, J. J. (1989) *Biochem. Biophys. Res. Commun. 166*, 667–672.

Fersht, A. R. (1977) Enzyme Structure & Mechanism, pp 95–96, W. H. Freeman, San Francisco.

Hart, K. W., Clarke, A. R., Wigley, D. B., Waldman, A. D. B., Chia, W. N., Barstow, D. A., Atkinson, T., Jones, J. B., & Holbrook, J. J. (1987) *Biochim. Biophys. Acta 914*, 294–298.

Holbrook, J. J., Liljas, A., Steindel, S. J., & Rossmann, M. G. (1975) The *Enzymes XIa*, 191–292.

Holbrook, J. J., Clarke, A. R., & Atkinson, T. (1989) U.K. Patent Application No. 8905269.0.

Holbrook, J. J., Wilks, H. M., & Clarke, A. R. (1992) U. K. Patent Application No. GB 9202033.8.

Hummel, W., Schutte, H., & Kula, M. R. (1988) *Anal. Biochem. 170*, 397–401.

Leatherbarrow, R. J. (1990) Grafit v.2.0 Erithracus Software Ltd., Staines, U.K.

Wendel, U., Hummel, W., & Langenbeck, U. (1989) *Anal. Biochem. 180*, 91–94.

Wigley, D. B., Gamblin, S. J., Turkenburg, J. P., Dodson, E. J., Piontek, K., Muirhead, H., & Holbrook, J. J. (1992) *J. Mol. Biol. 223*, 317–335.

Wilks, H. M., Hart, K. W., Feeney, R., Dunn, C. R., Muirhead, H., Chia, W. N., Barstow, D. A., Atkinson, T., Clarke, A. R., & Holbrook, J. J. (1988) *Science 242*, 1541–4.

Wilks, H. M., Halsall, D. J., Atkinson, T., Chia, W. N., Clarke, A. R., & Holbrook, J. J. (1990) *Biochemistry 29*, 8587–91.

Wu, J. T. (1991) *Ann. Clin. Lab. Sci. 21*, 123–142.